Geophysical Research Letters

RESEARCH LETTER
10.1029/2022GL100117

Routine Reversal of the AMOC in an Ocean Model Ensemble

William K. Dewar[1,2], Rhys Parfitt[1], and Nicolas Wienders[1]

[1]Department of Earth, Ocean and Atmospheric Science, Florida State University, Tallahassee, FL, USA, [2]Universite Grenoble Alpes, CNRS, IRD, Grenoble-INP, Institut des Geosciences de l'Environnement, Grenoble, France

Key Points:

- The Atlantic Meridional Overturning Circulation can reverse in sign
- Reversals appear in the annual cycle
- The reversals are the result of atmospheric forcing

Supporting Information:

Supporting Information may be found in the online version of this article.

Correspondence to:

W. K. Dewar,
wdewar@fsu.edu

Citation:

Dewar, W. K., Parfitt, R., & Wienders, N. (2022). Routine reversal of the AMOC in an ocean model ensemble. *Geophysical Research Letters*, *49*, e2022GL100117. https://doi.org/10.1029/2022GL100117

Received 23 JUN 2022
Accepted 6 DEC 2022

Author Contributions:

Conceptualization: William K. Dewar, Rhys Parfitt, Nicolas Wienders
Data curation: Nicolas Wienders
Formal analysis: William K. Dewar, Rhys Parfitt, Nicolas Wienders
Funding acquisition: Rhys Parfitt
Investigation: Nicolas Wienders
Methodology: William K. Dewar, Rhys Parfitt, Nicolas Wienders
Project Administration: Rhys Parfitt
Software: Nicolas Wienders
Visualization: Nicolas Wienders
Writing – original draft: William K. Dewar, Rhys Parfitt, Nicolas Wienders
Writing – review & editing: William K. Dewar, Rhys Parfitt, Nicolas Wienders

Abstract We describe a form of Atlantic Meridional Overturning Circulation (AMOC) variability that we believe has not previously appeared in observations or models. It is found in an ensemble of eddy-resolving North Atlantic simulations that the AMOC frequently reverses in sign at ~35°N with gyre-wide anomalies in size and that reach throughout the water column. The duration of each reversal is roughly 1 month. The reversals are part of the annual AMOC cycle occurring in boreal winter, although not all years feature an actual reversal in sign. The occurrence of the reversals appears in our ensemble mean, suggesting it is a forced feature of the circulation. A partial explanation is found in an Ekman response to wind stress anomalies. Model ensemble simulations run with different combinations of climatological and realistic forcings argue that it is the atmospheric forcing specifically that results in the reversals, despite the signals extending into the deep ocean.

Plain Language Summary The Atlantic Meridional Overturning Circulation (AMOC) is a climatically important component of the ocean circulation. It is routinely thought to flow northward at the surface and southward at depths of 2,000–3,000 m. Here we show that a significant component of the annual AMOC cycles are intervals during which it actually reverses this sense of flow and argue further that this is a response of the AMOC to the atmosphere. The AMOC anomaly is basin scale in size and extends over the full depth. These results have implications for annual heat storage in the North Atlantic.

1. Introduction

The Atlantic Meridional Overturning Circulation (AMOC) is a principal component of the global climate system. Defined as the basin-wide northward transport as a function of depth, it is the Atlantic part of the global conveyor belt circulation that couples all the ocean basins together and eventually flushes the deep ocean interior. Given its role in heat transport, the AMOC has been the subject of intense recent observational efforts, including the RAPID-MOCHA (Cunningham et al., 2007), MOVE (Send et al., 2011), SAMBA (Meinen et al., 2018), and OSNAP (Lozier et al., 2019) campaigns. These observations show that the AMOC is a highly variable feature spanning multiple timescales (e.g., Smeed et al., 2014), and several recent publications have addressed whether the AMOC is demonstrating any observable trends (e.g., Danabasoglu et al., 2021; Longworth et al., 2011). Central to answering this question is determining the nature of the AMOC variability; specifically whether AMOC variations are primarily the result of external atmospheric forcing, or if the AMOC is capable of its own intrinsic and hence unpredictable variability. If the latter is true, quantifying the strength of this variability becomes key to interpreting observations. We have been involved in a modeling study designed to address this question by generating an ensemble of eddy-resolving North Atlantic simulations and analyzing the ensemble mean and variations about that mean. The purpose of this paper is to describe the occurrence of a novel form of AMOC variability in our simulations that we believe has not previously been reported, either in observations or models. It is nonetheless robust across our ensemble and sufficiently surprising in its structure that we feel revealing it to the broader oceanographic community is warranted.

Analysis of RAPID observational time-series have previously demonstrated a strong annual cycle in AMOC variability at 26°N with minima in transport during boreal winter (Kanzow et al., 2010), a feature that is well-represented in models (e.g., Duchez et al., 2014). This annual variability has also been inferred at latitudes in the tropics and mid-latitudes in both observations (e.g., Herrford et al., 2021) and models (e.g., Hirschi et al., 2007). In our ensemble model simulations, we similarly identify notable minima in AMOC transport during boreal winter, however we find that the seasonal anomalies in the North Atlantic AMOC are often severe enough to generate large reversals in sign in the mid-latitudes. These reversals are basin scale in size, encompassing the north-south extent of the subtropical gyre, reach throughout the entirety of the water column, persist for a month to 6 weeks, and have a strong preference for winter occurrences. As the occurrence of these reversals appears

in the ensemble mean AMOC, they are suggested to be a feature responding to model forcing. While the reversals themselves are beset with intrinsic oceanic variability, the strength of the associated intrinsic variations (± 5 Sv) are considerably less than the ensemble mean signal (∼20 Sv). In Section 2, a description of the model ensemble simulations is provided. In Section 3, the phenomenon of the AMOC reversals is documented and a leading order explanation in terms of Ekman response is given, whilst a discussion regarding implications and next steps are given in Section 4.

2. Model Description

The results in this article derive from a 24-member ensemble simulation (our "Ocean Realistic, Atmosphere Realistic" simulation, ORAR) performed with the Massachusetts Institute of Technology General Circulation Model (Marshall et al., 1997), set up in the Atlantic between 20°S and 55°N. The model runs are performed at an "eddy-resolving" horizontal resolution of (1/12)°, and there are 46 vertical layers ranging from thicknesses of 6–250 m. A 55-year, (1/12)° horizontal resolution, ocean-only global configuration ORCA12.L46-MJM88 (Molines et al., 2014; Sérazin et al., 2015), is used for open boundary conditions at the northern and southern boundaries, and at the Strait of Gibraltar. An atmospheric boundary layer model is coupled to the ocean model at the surface (CheapAML, Deremble et al., 2013), in order to better represent air-sea exchanges and avoid the suppression of surface ocean dynamics caused by a prescribed atmosphere. The configuration is integrated for 50 years (1963–2012). Initial conditions are constructed from 1-year-long simulations initialized from 24 alternative days, whereby the 24 oceanic states at the end of these 1-year-long simulations were used to initialize the ensemble members. Oceanic data output is provided every 5 days, where each variable represents the 5-day average centered on the output date. The model output of the above simulations has been compared to observational output from RAPID-MOCHA in Jamet et al. (2019b), where it was shown that both the simulated and observed signals agree well, especially so at near annual frequencies. The atmospheric conditions fed to CheapAML are provided every 6 hr, and linear interpolation is used to fill in at intervening time steps. Further details on the ORAR model ensemble and comparison with observations appear in Jamet et al. (2019a, 2019b).

In addition to the above simulations, we have also generated ensembles of the same temporal length, but subject to various combinations of climatological and realistic forcings. While our most realistic ORAR simulations apply full atmospheric variability and fully variable boundary conditions, other combinations include climatological atmospheric states with variable ocean boundary conditions at the northern, southern and Mediterranean outflow boundaries (ORAC, Ocean Realistic, Atmosphere Climatology, 12-member), vice versa (OCAR, Ocean Climatology, Atmosphere Realistic, 12-member) and climatological forcing conditions of all types (OCAC, 24-member). For clarity, runs with a climatological atmosphere are actually subject to a "repeating year" whereby the atmospheric forcing repeats the 1 July 2002 to 30 June 2003 conditions. This year was chosen specifically as it was both relatively neutral with regards to the North Atlantic Oscillation and the El Nino-Southern Oscillation, and the choice to repeat from summer to summer was to limit any impacts of the jump to the summertime mixed layer depth, which is shallow relative to that in the winter.

3. Results

We interpret an ensemble as a collection of equally plausible dynamical states of the North Atlantic, from which it is impossible to declare a "winner", that is, to select from the group of simulations one that is the correct simulation. Inasmuch as each member has responded to externally applied inputs in the form of applied boundary conditions and atmospheric states, each has a forced component and a residual that reflects the internal capacity of the system to generate intrinsic variability. This allows to separate the "forced" response of the system (i.e., that due to the atmosphere and the boundary conditions) from the "chaotic" response of the system by computing the ensemble mean

$$< u >= \frac{1}{N} \sum_{i=1}^{N} u_i \quad (1)$$

where the index i denotes the ith member of a collection of size N and u is any variable from the model. In the case of the AMOC, we work with north-south transport as a function of depth and longitude. The AMOC overturning stream function, $\psi(\lambda, z)$ where λ is latitude and z depth, is given by

$$\psi(\lambda, z) = \int_{\theta_w}^{\theta_e} \int_{z_b}^{z} v(\lambda, \theta, z) \cos(\lambda) a d z d \theta \quad (2)$$

where v is meridional velocity, z_b is bottom depth, a is the earth radius and θ is longitude. Ensemble averaging over all ORAR members returns the ORAR ensemble and temporal mean AMOC streamfunction, which appears in Figure 1. It is dominated by a poleward surface flow returning at roughly 2,500 m, which is the North Atlantic Deep Water (NADW) cell of the AMOC. The center of this cell is at roughly 1 km depth. At the bottom is the poleward flowing Antarctic Bottom Water, again returning southward at mid-depth. This is a very standard looking model-based AMOC streamfunction (e.g., Hirschi et al., 2020).

The strength of the upper cell is approximately 17 Sv, although the maximum amplitude varies as a function of latitude. Of note is the pronounced maximum overturning observed at roughly 36N and at a depth of 1 km, which coincides with the predominant location of the separated Gulf Stream axis. As is well known, the AMOC strength varies in time, and this location is recognized to be a region of strong variability in AMOC transport on sub-annual timescales, especially in models classified as "eddy-resolving" (Hirschi et al., 2020). The absolute maximum of the AMOC cell usually occurs at the boxed location in Figure 1a, although it does move around in time and its detailed location differs amongst the ensemble members. Accordingly, as a measure of AMOC variability, we define an AMOC index by averaging the streamfunction value in a 5° by 1,100 m box centered roughly on (34.2 N, –1,292 m) for each ensemble member at each timestep. A plot of the 50-year time-series of the AMOC index for all members appears in the upper panel of Figure 1b. In addition, Figure 1c contains the AMOC index for the ORAR ensemble mean, whereas Figure 1d contains the variability about the mean (see Equation 1).

Figure 1b demonstrates that the AMOC transport in our region of interest is characterized by the repeated occurrence of anomalously low and negative AMOC values. These minima in the AMOC are seasonal in nature and occur in boreal winter. While the AMOC is typically found in its classical northward state, it is not unusual for these minima to reverse the main cell at the surface from northward to southward. If we take a vanishing value for overturning as a threshold, we find that 70% of the years (35 out of 50) exhibit a reversal in AMOC transport in at least one ORAR member in Figure 1b. If we restrict our view to the ORAR ensemble mean in Figure 1c, this fraction reduces to 40% (20 out of 50). The plot of index values associated with the intrinsic variability in Figure 1d shows no extreme values during the reversals. This is consistent with the intrinsic variability being insensitive to the reversals and indicates that the primary signal associated with these anomalous minima and reversals is found in the ensemble mean. This is further supported by a spectral analysis, discussed later. We interpret the ocean response to the model forcing to be the fundamental reason for the appearance of these minima and reversals, although intrinsic ocean variability is also an important component in any actual realization.

A natural question also arises about the "typical" AMOC structure associated with these minima and reversals. In response, Figure 2 illustrates a composite of extreme reversal events. In this figure, we isolate all those intervals during which the ORAR ensemble mean AMOC index is less than −10 Sv, center the composite event time on the minimum value of the index and average together all such realizations. In addition, 20-day lead and lag composites are included at 5-day intervals prior to and after the extrema to describe the variability of these events. Perhaps the most noticeable aspect of these plots is the breadth of the reversal at the extrema. This occurs in the middle panel of Figure 2, which illustrates that extreme reversals extend meridionally throughout the subtropical gyre (∼20°N–40°N) and throughout the water column. The upper NADW clockwise cell collapses, and the upper AMOC circulation joins with the counter-clockwise Antarctic Bottom Water Cell. The overall structure persists for less extreme choices for the minimum, for example, minima less than 0 or −5 Sv, with the primary difference being that the negative streamfunction value at 1,000 m becomes less extreme, while the surface and deep anomalies are relatively unaffected by the choice (not shown). The sequence in Figure 2 suggests a roughly 40 days time scale, from the initial onset to its subsequent disappearance.

The seasonal nature of these events is reinforced in the ORAR index power spectrum in Figure 3a. The spectrum itself is largely unremarkable except for the pronounced spike at the annual period, which is two orders of magnitude larger than for all other values. Naturally, spectral spikes at the annual period are not unusual, however the time-series derive from a depth of more than one km, beneath where any obvious direct seasonal influence, such as Ekman transport, reaches. The interpretation that these annual events is due to the model forcing is emphasized in the power spectrum of the AMOC index intrinsic variability in Figure 3b. This is calculated as the average of

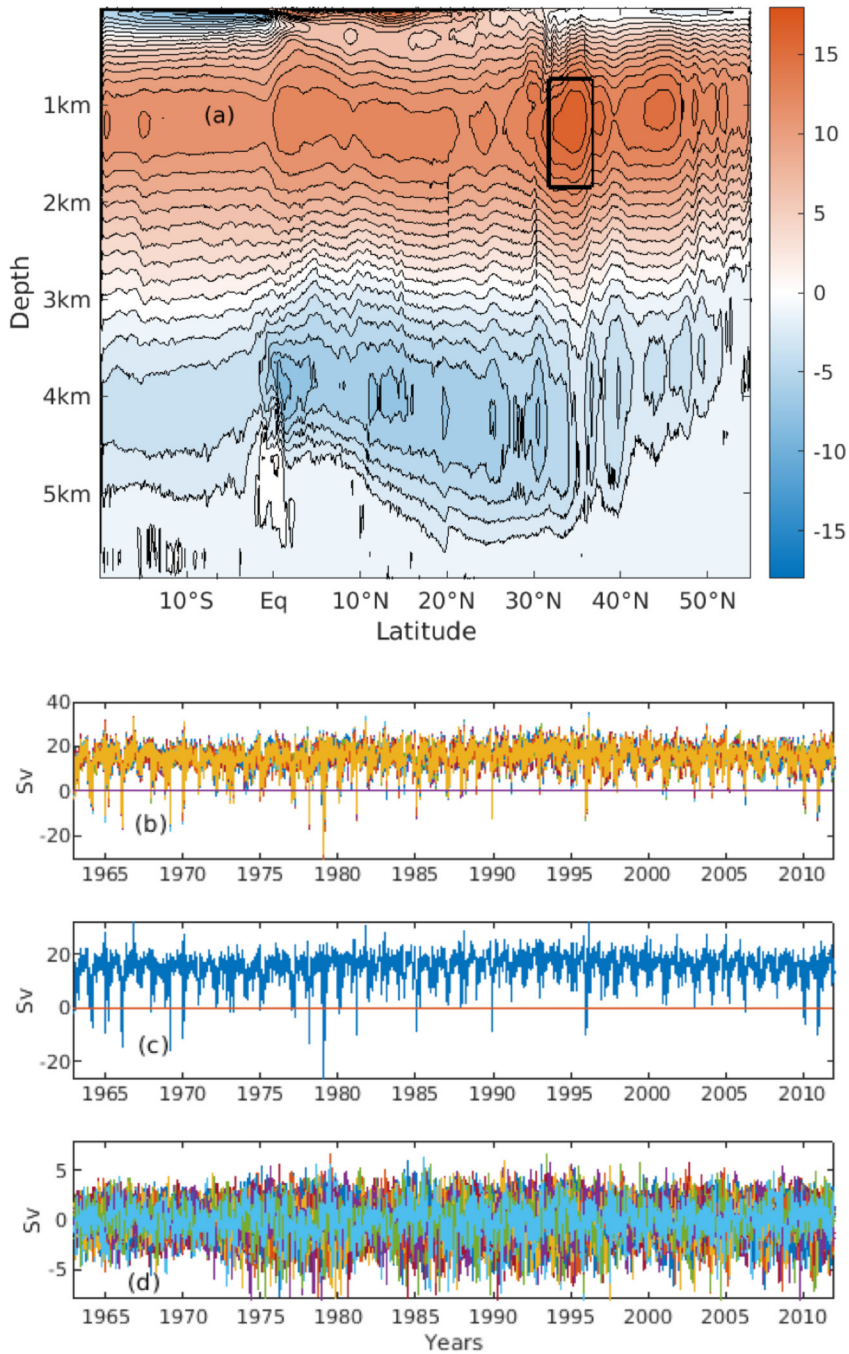

Figure 1. (a) Atlantic Meridional Overturning Circulation (AMOC) time and ensemble averaged overturning streamfunction as a function of depth and latitude in the North Atlantic in the ORAR simulations (contours and color bar in Sv). The area between latitudes 31.7°N and 36.7 N and depths 734 and 1850 m is the box over which we generate our averaged AMOC index. Fifty-year timeseries of our AMOC are shown in (b) for all 24 ORAR ensemble members and (c) for the ORAR ensemble mean. The variation of each ensemble member from the ensemble mean is shown in (d).

the individual power spectra of each ORAR ensemble member. In this plot, the annual period does not appear as a distinguished frequency and the low frequency structure at periods beyond 1 year is largely indistinguishable from white. It is noted that the robustness of these annual minima and reversals has been tested by developing other AMOC indices, such as the average of the AMOC overturning streamfunction in a 470 m thick box centered at 1,200 m depth, stretching from 20°N to 37°N. Similar results were noted using each of these indices (see Supporting Information S1).

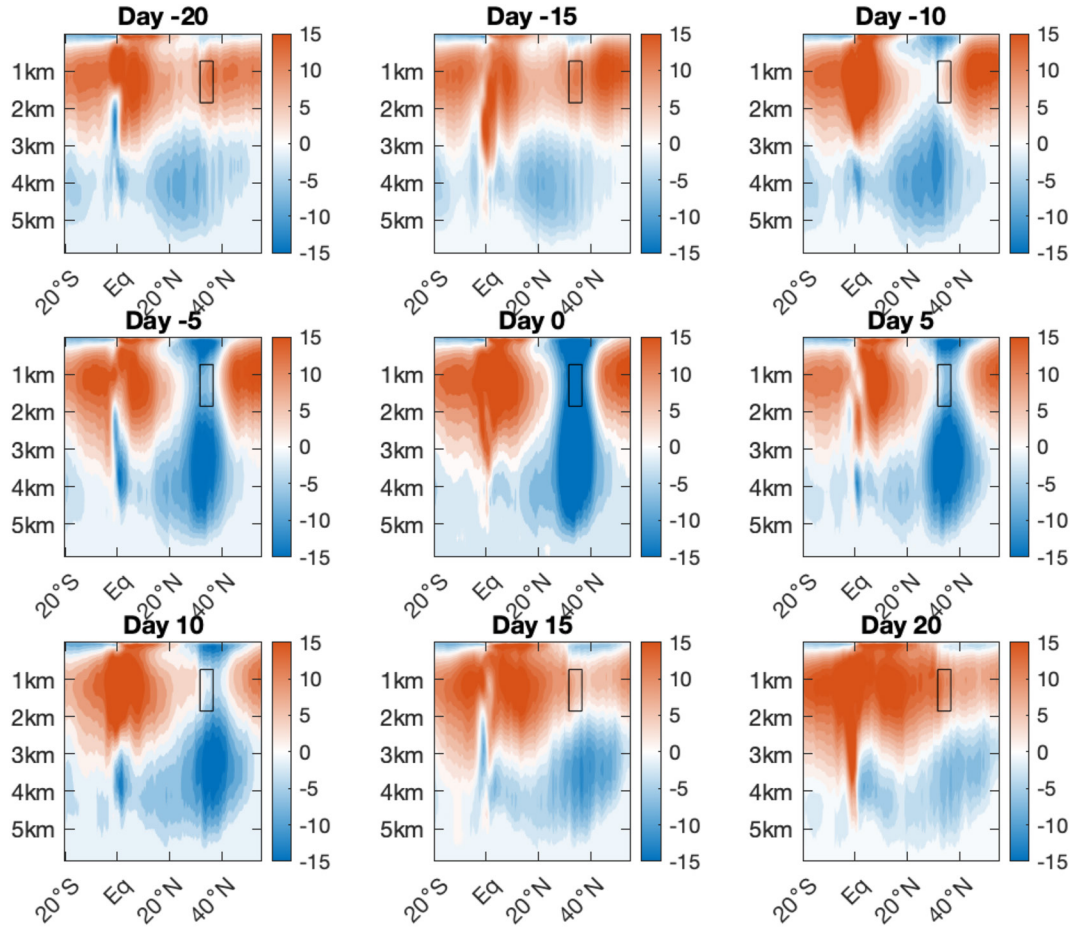

Figure 2. Two-dimensional composite mean structure of extreme reversal events in the ORAR ensemble mean (colorbars in Sv). All such occurrences with minimum less than −10 Sv were used. The upper left panel shows conditions prior to the extreme, and successive panels moving left to right and top to bottom show structure at intervals of 5 days.

Lastly, given the interpretation that model forcing is responsible for the reversals, it is reasonable to ask which component of the model forcing is most significant. As such, Figures 4a–4c illustrate the 50-year timeseries of our AMOC index, for each of the members associated with the (a) OCAC (b) OCAR, and (c) ORAC simulations. The annual cycle, in which minima in AMOC transport occur in boreal winter, are present in all three simulations. However, significant variability in the magnitude of these minima, as well as significant reversals in the AMOC, can only be found in the OCAR simulations with the realistic atmospheric forcing. Indeed, Figure 4b closely resembles Figure 1a. Conversely, the annual minima in the OCAC and ORAC climatological atmosphere simulations appear relatively consistent from year-to-year. Comparison of the annual cycles between the OCAC and ORAC simulations suggest that realistic oceanic forcing has a relatively muted impact (~±1 Sv) relative to that of the atmosphere (±15 Sv). While differences are expected due to intrinsic variability, those clearly do not change the fundamental annual AMOC cycle. Taken in sum, these plots argue the presence of the weakening, and in particular its tendency for intervals of reversal, is due to atmospheric forcing.

The structure of the atmospheric forcing associated with strong AMOC reversals is illustrated in Figure 4d, which plots the composite wind anomalies associated with reversals in our AMOC index for values less than −5 Sv in our ORAR simulations. Anomalies for an individual event are calculated as the departure from the 50-year ensemble mean at the time of that individual event, before all anomalies are averaged together. The composite wind anomalies illustrate that AMOC reversals are associated with anomalous atmospheric cyclonic circulation in the central North Atlantic around ~(42°W, 48°N), that results in increased westerly wind speeds of up to ~10 ms^{-1} across most of our model domain (25°N–45°N) and decreases up to 5 ms^{-1} at ~50°N.

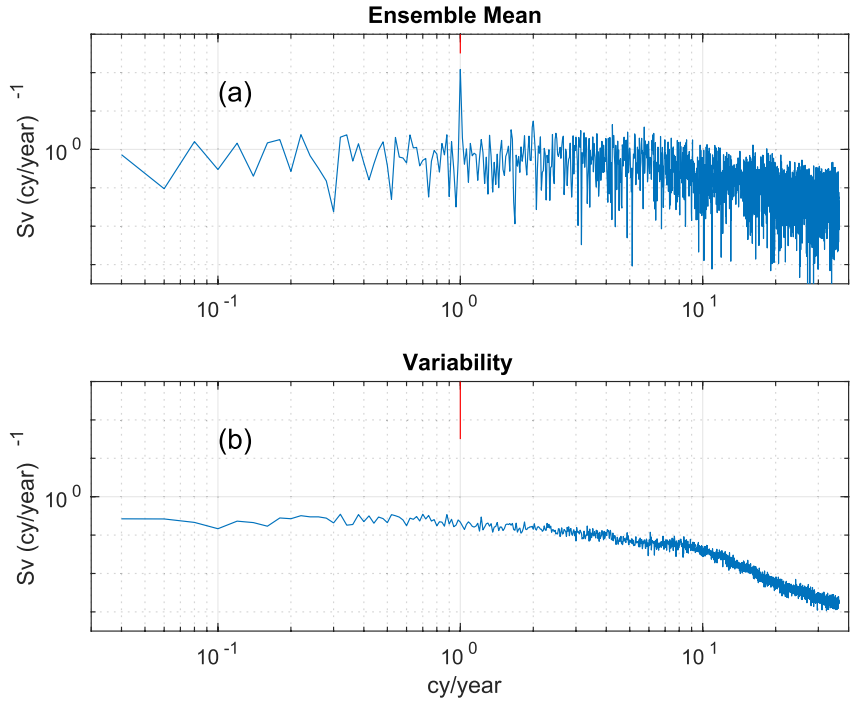

Figure 3. (a) Spectrum of the ORAR ensemble mean Atlantic Meridional Overturning Circulation (AMOC) index from Figure 1c. (b) Spectrum of the AMOC index intrinsic variability from Figure 1d. The red line marks 1 cy/yr.

Anomalously strong wind-stress combined with the short event duration suggests combined Ekman transport, barotropic dynamics are at play. Jayne and Marotzke (2001) and Killworth (2008) argue high frequency wind anomalies drive a net Ekman transport anomaly that is compensated barotropically. We have examined the role of this Ekman cell (see Supporting Information S1 for details) and show the residual overturning streamfunction after the cell has been removed in Figure 5. Most notably, the cell accounts for most of the overturning anomaly at the event extreme, but still leaves a net anomaly. Specifically, the mean overturning in the index box is roughly 17 Sv, and the composite value during the reversals is −15 Sv. Removing the Ekman contribution returns an index value of roughly 2 Sv, or about half of the anomaly. On the other hand, the index after Ekman cell removal still displays reversals 10% of the time (5 years out of 50, not shown).

We interpret the residual as due to a more complicated barotropic response than instant compensation, likely representing the bottom topography through which the barotropic response must propagate. More definitive statements than this await further study.

4. Discussion

This study has investigated the nature of the annual cycle in the North Atlantic AMOC transport in a North Atlantic eddy-resolving model ensemble simulation with realistic oceanic and atmospheric forcing. It is found that the AMOC transport between 30°N and 40°N exhibits a pronounced annual cycle, with distinct minima in transport in boreal winter, in line with previous studies. This annual cycle is found to be a property of the ensemble mean, suggesting that it is primarily a product of the model forcing. Strikingly, in our model ensemble simulation the minima associated with the annual cycle are often strong enough to result in strong reversals in AMOC transport (up to ∼−20 Sv) between 30°N and 40°N. Furthermore, these reversals are basin-scale, extend throughout the water column and have a duration of roughly ∼40 days, with a strong preference for winter occurrences. Further investigation using model ensembles with combinations of climatological and realistic forcings suggest that the sharp AMOC weakening associated with the annual cycle, and in particular those that result in deep reversals, owe their existence to atmospheric forcing. Composites at times of AMOC reversals highlight an associated anomalous cyclonic circulation in the central North Atlantic with significantly enhanced westerlies across most

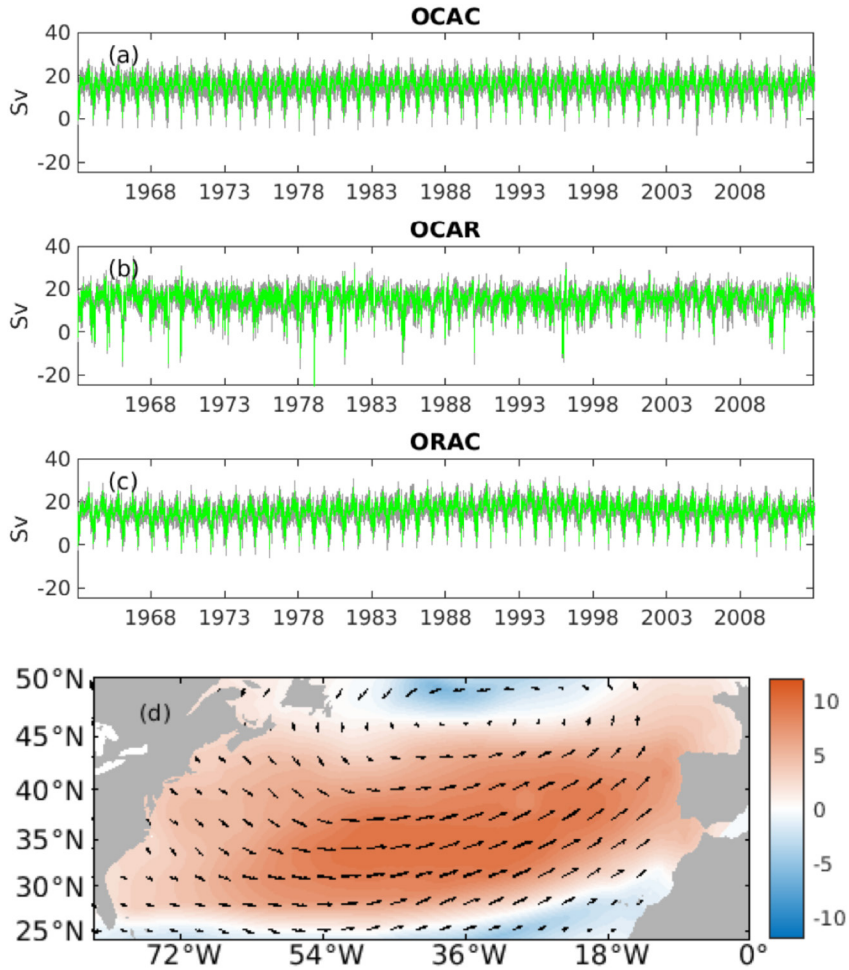

Figure 4. Time-series associated with each member of the model ensemble simulations that mix climatological (C), realistic (R), atmospheric (A) and oceanic (O) forcings: (a) OCAC (b) OCAR and (c) ORAC. The means are in green and the gray lines are the ensemble members. (d) The anomalous wind field (anomalous speed (m/s) in shading, direction as vectors) at times when the Atlantic Meridional Overturning Circulation index in the ORAR ensemble mean is lower than −5 Sv.

of the model domain. Allowing for a simple compensated Ekman cell explains a considerable fraction of the anomaly, but leaves behind a residual probably associated with a more subtle barotropic response.

To our knowledge, neither observational nor modeling studies have indicated the presence of significant reversals in the AMOC from 30 to 40°N previously. Nevertheless, analyses of our full North Atlantic model ensemble AMOC variability have indicated a significant agreement with observational estimates at various latitudes, particularly at sub-annual frequencies (e.g., Jamet et al., 2019a). Such inconsistencies motivate the need for further observational campaigns to fully validate and understand differences in model simulations of the AMOC.

Note also the wintertime subtropical North Atlantic transfers a large amount of heat to the atmosphere (Yu & Weller, 2007), with the most extreme ocean-atmosphere events known to critically impact the development of weather systems (e.g., Hirata et al., 2019; Parfitt & Kwon, 2020). The reversals in Figure 2 imply the reoccurrence of strong upper ocean heat convergence anomalies in the wintertime subtropical gyre, providing potential feedback between atmospheric-driven sub-annual AMOC and atmospheric variability. Irrespective of this however, the results of these model ensemble simulations clearly indicate that the atmosphere is the primary control on the magnitude of the AMOC annual cycle, and also support previous suggestions that the atmospheric impact on the AMOC extends well into the ocean interior (e.g., Duchez et al., 2014).

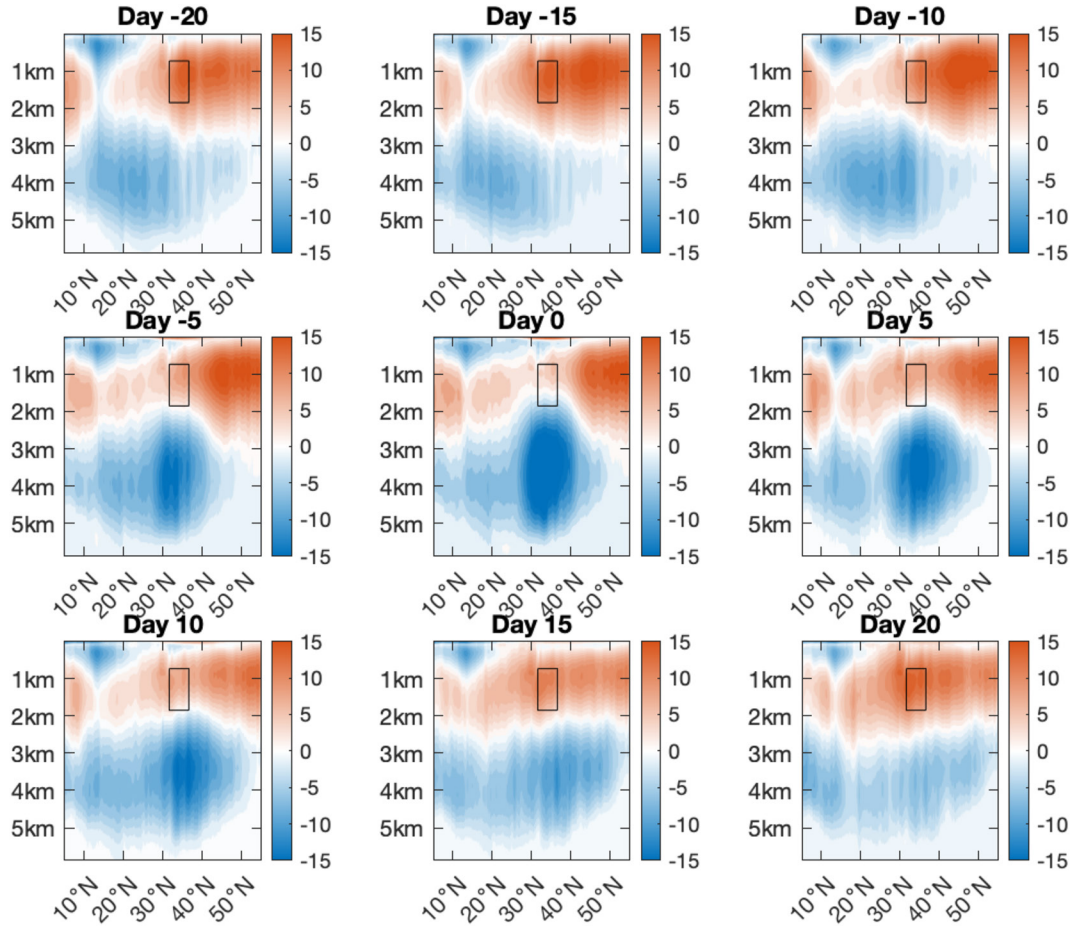

Figure 5. Adjusted overturning streamfunction composited from reversals with anomalies more than −10 Sv, consisting of the total Atlantic Meridional Overturning Circulation streamfunction with the Ekman cell removed. The presentation is as in Figure 2. Note that the negative anomaly in the upper 2 km has been accounted for, but an anomalous overturning cell remains, and a negative anomaly remains in the deep ocean.

Data Availability Statement

The data in this study are available at https://doi.org/10.6084/m9.figshare.19610223.v1.

Acknowledgments
This research was funded by the National Science Foundation through Grants OCE-2023585 and OCE-2123632. This manuscript has benefitted greatly from a thorough exchange with two anonymous reviewers. Their efforts are muchly appreciated.

References

Cunningham, S. A., Kanzow, T., Rayner, D., Baringer, M., Johns, W., Marotzke, J., et al. (2007). Temporal variability of the Atlantic meridional overturning circulation at 26.5°N. *Science*, *317*(5840), 935–938. https://doi.org/10.1126/science.1141304

Danabasoglu, G., Castruccio, F. S., Small, R. J., Tomas, R., Frajka-Williams, E., & Lankhorst, M. (2021). Revisiting AMOC transport estimates from observations and models. *Geophysical Research Letters*, *48*(10), e2021GL093045. https://doi.org/10.1029/2021gl093045

Deremble, B., Wienders, N., & Dewar, W. (2013). CheapAML: A simple, atmospheric boundary layer model for use in ocean-only model calculations. *Monthly Weather Review*, *141*(2), 809–821. https://doi.org/10.1175/mwr-d-11-00254.1

Duchez, A., Hirschi, J. M., Cunningham, S. A., Blaker, A. T., Bryden, H. L., de Cuevas, B., et al. (2014). A new index for the Atlantic meridional overturning circulation at 26°N. *Journal of Climate*, *27*(17), 6439–6455. https://doi.org/10.1175/jcli-d-13-00052.1

Herrford, J., Brandt, P., Kanzow, T., Hummels, R., Araujo, M., & Durgadoo, J. V. (2021). Seasonal variability of the Atlantic Meridional Overturning Circulation at 11 S inferred from bottom pressure measurements. *Ocean Science*, *17*(1), 265–284. https://doi.org/10.5194/os-17-265-2021

Hirata, H., Kawamura, R., Nonaka, M., & Tsuboki, K. (2019). Significant impact of heat supply from the Gulf Stream on a "superbomb" cyclone in January 2018. *Geophysical Research Letters*, *46*(13), 7718–7725. https://doi.org/10.1029/2019gl082995

Hirschi, J. J., Killworth, P. D., & Blundell, J. R. (2007). Subannual, seasonal, and interannual variability of the North Atlantic meridional overturning circulation. *Journal of Physical Oceanography*, *37*(5), 1246–1265. https://doi.org/10.1175/jpo3049.1

Hirschi, J. J. M., Barnier, B., Böning, C., Biastoch, A., Blaker, A. T., Coward, A., et al. (2020). The Atlantic meridional overturning circulation in high-resolution models. *Journal of Geophysical Research: Oceans*, *125*(4), e2019JC015522. https://doi.org/10.1029/2019jc015522

Jamet, Q., Dewar, W. K., Wienders, N., & Deremble, B. (2019a). Fast warming of the surface ocean under a climatological scenario. *Geophysical Research Letters*, *46*(7), 3871–3879. https://doi.org/10.1029/2019gl082336

Jamet, Q., Dewar, W. K., Wienders, N., & Deremble, B. (2019b). Spatiotemporal patterns of chaos in the Atlantic overturning circulation. *Geophysical Research Letters*, *46*(13), 7509–7517. https://doi.org/10.1029/2019gl082552

Jayne, S., & Marotzke, J. (2001). The dynamics of ocean heat transport variability. *Reviews of Geophysics*, *39*(3), 385–411. https://doi.org/10.1029/2000rg000084

Kanzow, T., Cunningham, S. A., Johns, W. E., Hirschi, J. J., Marotzke, J., Baringer, M. O., et al. (2010). Seasonal variability of the Atlantic meridional overturning circulation at 26.5°N. *Journal of Climate*, *23*(21), 5678–5698. https://doi.org/10.1175/2010jcli3389.1

Killworth, P. (2008). A simple linear model of the depth dependence of the wind-driven variability of the Meridional Overturning Circulation. *Journal of Physical Oceanography*, *38*(2), 492–502. https://doi.org/10.1175/2007jpo3811.1

Longworth, H. R., Bryden, H. L., & Baringer, M. O. (2011). Historical variability in Atlantic meridional baroclinic transport at 26.5°N from boundary dynamic height observations. *Deep-Sea Research, Part II*, *58*(17–18), 1754–1767. https://doi.org/10.1016/j.dsr2.2010.10.057

Lozier, M. S., Li, F., Bacon, S., Bahr, F., Bower, A. S., Cunningham, S. A., et al. (2019). A sea change in our view of overturning in the subpolar North Atlantic. *Science*, *363*(6426), 516–521. https://doi.org/10.1126/science.aau6592

Marshall, J., Adcroft, A., Hill, C., Perelman, L., & Heisey, C. (1997). A finite-volume, incompressible Navier Stokes model for studies of the ocean on parallel computers. *Journal of Geophysical Research*, *102*(C3), 5753–5766. https://doi.org/10.1029/96jc02775

Meinen, C., Speich, S., Piola, A., Ansorge, I., Campos, E., Kersalé, M., et al. (2018). Meridional overturning circulation transport variability at 34.5°S during 2009–2017: Baroclinic and barotropic flows and the dueling influence of the boundaries. *Geophysical Research Letters*, *45*(9), 4180–4188. https://doi.org/10.1029/2018GL077408

Molines, J., Barnier, B., Penduff, T., Treguier, A., & Le Sommer, J. (2014). ORCA12. L46 climatological and interannual simulations forced with DFS4. 4: GJM02 and MJM88. In *Drakkar group experiment rep (GDRI-DRAKKAR-2014-03-19)*. Retrieved from http://www.drakkar-ocean.eu/publications/reports/orca12_reference_experiments_2014

Parfitt, R., & Kwon, Y. (2020). The modulation of Gulf Stream influence on the troposphere by the eddy-driven jet. *Journal of Climate*, *33*(10), 4109–4120. https://doi.org/10.1175/jcli-d-19-0294.1

Send, U., Lankhorst, M., & Kanzow, T. (2011). Observation of decadal change in the Atlantic meridional overturning circulation using 10 years of continuous transport data. *Geophysical Research Letters*, *38*(24), 24606. https://doi.org/10.1029/2011GL049801

Sérazin, G., Penduff, T., Grégorio, S., Barnier, B., Molines, J. M., & Terray, L. (2015). Intrinsic variability of sea level from global ocean simulations: Spatiotemporal scales. *Journal of Climate*, *28*(10), 4279–4292. https://doi.org/10.1175/jcli-d-14-00554.1

Smeed, D. A., McCarthy, G. D., Cunningham, S. A., Frajka-Williams, E., Rayner, D., Johns, W. E., et al. (2014). Observed decline of the Atlantic meridional overturning circulation 2004–2012. *Ocean Science*, *10*(1), 29–38. https://doi.org/10.5194/os-10-29-2014

Yu, L., & Weller, R. (2007). Obectively analyzed air-sea heat fluxes for the global ice-free oceans (1981–2005). *Bulletin of the American Meteorological Society*, *99*(4), 527–540. https://doi.org/10.1175/bams-88-4-527